Synthesis and Post-Processing of Chemically Homogeneous Nanothreads from 2,5-Furandicarboxylic Acid

Samuel G. Dunning,[1]* Bo Chen,[2,3] Li Zhu,[4] George D. Cody,[1] Stella Chariton,[5] Vitali B. Prakapenka,[5] Dongzhou Zhang,[6] and Timothy A. Strobel[1]*

[1] Earth and Planets Laboratory, Carnegie Institution for Science, Washington, District of Columbia 20015, United States
[2] Donostia International Physics Center, Paseo Manuel de Lardizabal, 4, 20018 Donostia-San Sebastian, Spain
[3] IKERBASQUE, Basque Foundation for Science, Plaza Euskadi 5, 48009 Bilbao, Spain
[4] Physics Department, Rutgers University-Newark, 101 Warren Street, Newark, NJ 07102, United States
[5] Center for Advanced Radiation Sources, The University of Chicago, Chicago, Illinois 60637, United States
[6] Hawaii Institute of Geophysics and Planetology, School of Ocean and Earth Science and Technology, University of Hawaii at Manoa, Honolulu, HI 96822, United States

*Correspondence: sdunning@carnegiescience.edu, tstrobel@carnegiescience.edu

Solid-state synthesis represents an alternative to solution-phase chemistry that can provide routes to materials typically unobtainable by conventional methods. However, multiple competing reaction pathways under high-pressure conditions makes the targeted synthesis of chemically homogeneous systems a challenge. Nanothreads, one-dimensional diamondoid polymers formed through the compression of aromatic hydrocarbons present a unique opportunity to carry out high pressure reactions in a controlled and predictable manner. We hypothesize that through careful consideration of molecular stacking and intermolecular forces (e.g., H-bonding), it is possible to form chemically homogeneous nanothreads that retain precisely located chemical functionality. Herein, we report the scalable solid-state polymerization of 2,5-furandicarboxylic acid through sequential [4 + 2] Diels Alder cycloaddition reactions. The resulting nanothread product is decorated with a high density of pendant carboxylate groups, presenting new opportunities for post-synthetic processing and functional applications. Transition metal coordination is demonstrated for the functionalized threads, representing proof-of-concept for the utilization of nanothreads as independent synthons and the possibility for novel, extended multidimensional networks.

While solution-based chemical synthesis is generalizable, controlled organic reactions in the solid state are notoriously challenging due to limitations such as geometrical/steric constraints and multiple energetically competitive pathways.[1-9] Nevertheless, generalized synthetic control of organic reactions in the solid state with precision comparable to traditional methods would enable a range of new chemical species and synthons that are challenging or impossible to obtain by solution-based chemistry.[10] High-pressure synthesis represents an emerging approach to control solid-state organic transformations that enables novel reactions to produce new structural motifs and novel bonding environments (e.g., sp^3 carbon-rich structures).[11-16]

Carbon nanothreads are a novel class of crystalline, one-dimensional sp^3 carbon nanomaterials formed at high pressure. Since the initial formation of polymeric nanothreads through the slow, anisotropic compression of benzene,[17] several synthetic strategies have been developed to limit the number of potential reaction pathways and promote the formation of chemically homogeneous products through selective cycloaddition.[18-24] As the backbones of nanothreads extend in only one direction, these ultrathin carbon materials are predicted to marry the superlative physical properties of diamond with the flexibility of traditional polymers.[25-30] The chemical composition of nanothreads can be precisely controlled through careful selection of small molecule precursors (e.g., benzene,[17,31] pyridine,[32] pyridazine[23]), giving them potential advantages over comparable nanomaterials (e.g., nanotubes). Therefore, the possible applications of nanothreads are diverse, including novel energy storage and advanced structural materials.[26,33,34]

However, the formation of ordered nanothreads containing homogeneous pendant functional groups remains a significant challenge. Under nanothread-forming conditions, pendant groups are prone to side reactions, which can produce a variety of bonding motifs. Such side reactions can result in the formation of chemically inhomogeneous materials, causing the loss of both long-range order and precise chemical functionality.[19,35] A reliable method of synthesizing nanothreads decorated with a high density of stable

functional groups would mark a significant advancement, creating new opportunities for post-synthetic nanothread modification, and the use of nanothreads as independent synthons for the formation of multidimensional frameworks with diamond-core scaffolds.

To enhance synthetic control over homogeneous functionalized nanothreads, we investigated pi-stacked, heteroatom-substituted aromatics with functional groups possessing stabilizing interactions. Furans were selected for the oxygen heteroatom substitution, which reduces aromaticity and can guide nanothread formation to a carbon exclusive reaction pathway, resulting in the formation of so-called "perfect" nanothreads.[20,21] Functional groups containing hydrogen bond donors/acceptors were chosen due to the strength of hydrogen-bonding interactions,[36] which we hypothesized would stabilize the geometry under compression and minimize potential intermolecular side reactions. In addition, carboxylic acids are key chemical building blocks, fundamental to diverse applications including drug discovery[37], superabsorbent polymers[38], porous material synthesis[39], food additives[40] and catalyst design.[41] Therefore, nanothreads with a high density of carboxylate groups are relevant to a wide range of post-processing reactions and potential applications.

Herein, we report the synthesis and characterization of a chemically homogeneous crystalline nanothread polymer, formed by the compression of 2,5-furandicarboxylic acid (2,5-FDCA). The resulting threads retain carboxylate functionality, allowing for post-processing of the nanothread material. The material readily absorbs ambient moisture and can be used to coordinate various 3*d* metal ions, opening the door to the use of nanothreads as building blocks for the formation of complex, multidimensional networks analogous to Metal Organic Frameworks (MOFs) and precise tuning of their physical properties.

RESULTS & DISCUSSION

2,5-furandicarboxylic acid (2,5-FDCA) crystallizes[42] with molecular pi-stacking suitable for a topochemical-type reaction pathway under compression (i.e., d_c < ~4 Å, Φ ~ 25°, see Fig. 1).[23,35] The ambient-pressure, closest-contact intermolecular C-C distances of 3.28 Å indicate that the system is a likely candidate to undergo a nanothread forming intermolecular [4 + 2] cycloaddition reaction, consistent with the known mechanism for furan nanothread formation as determined by solid-state NMR studies.[20] While similar reactions from precursors containing pendant functional groups typically result in the formation of chemically diverse nanothreads due to unwanted side reactions between pendant groups,[19,35] the carboxylate groups in 2,5-FDCA are stabilized in a hydrogen-bonding network along the crystallographic *b*-axis, which we hypothesize to preserve precise functionalization during cycloaddition along the carbon backbone.

.

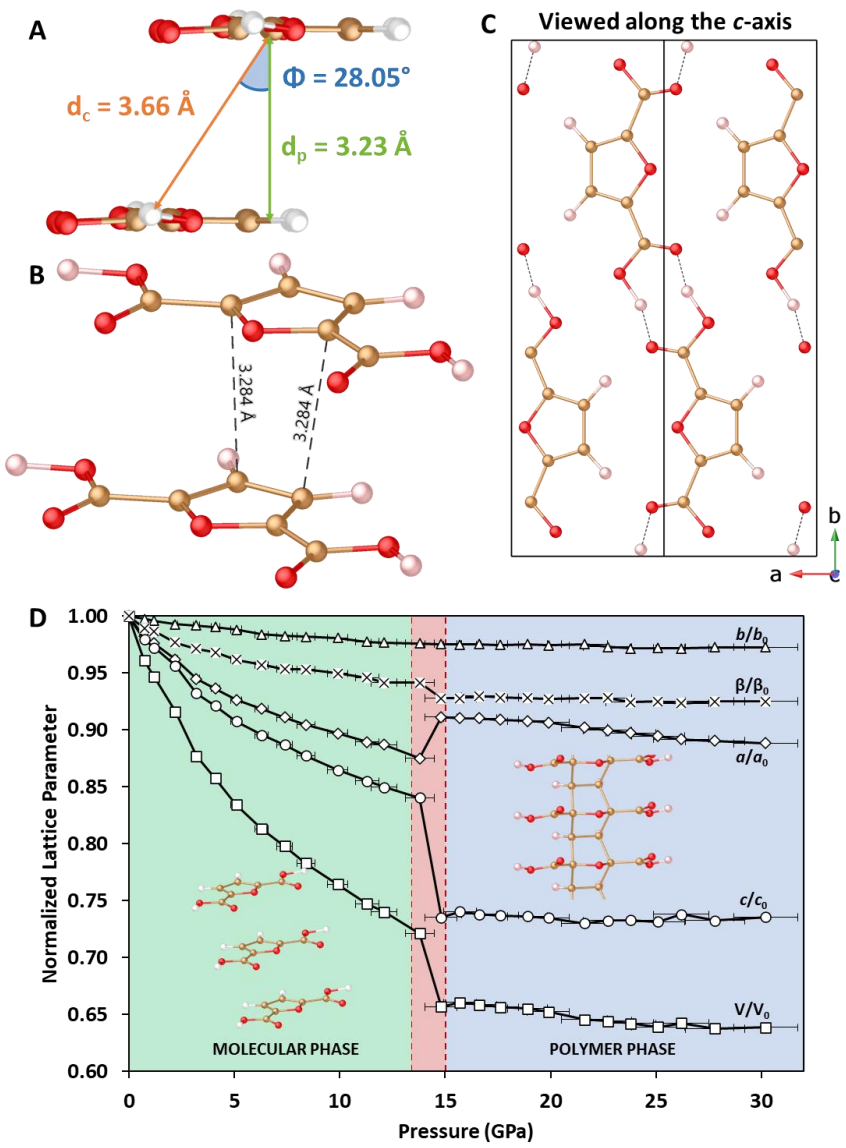

Figure 1. Structural Arrangement and Evidence for the Proposed Polymerization of 2,5-FDCA
A) Starting molecular structure of 2,5-furandicarboxylic acid (2,5-FDCA) showing local π-stacking at ambient. d_c is the centroid distance between rings, d_p is the distance between parallel planes, φ is the slippage angle between ring centroids, defined by the ring normal and centroid vectors; B) Nearest-neighbor [4 + 2] cycloaddition pathway C) View of 2,5-FDCA along the molecular stacking c-axis; D) Comparison of relative changes in unit cell parameters s as a function of pressure.

To monitor the reaction experimentally, ground powders and single-crystals of 2,5-FDCA were loaded into diamond anvil cells (DACs) and compressed to pressures up to 30 GPa while the structure and bonding of the sample was monitored in situ using a combination of X-ray diffraction (XRD) and vibrational spectroscopy. XRD patterns of the powder sample agree with the reported structure and all patterns were readily indexed to a monoclinic $P2_1/m$ cell (Fig 1D).[42] During compression, reflections monotonically shift to lower d-spacings consistent with a pressure-induced contraction of the unit cell (Fig. S1). Above 13 GPa, a 9% drop in the unit cell volume, associated with a large decrease in the molecular stacking (*c*-axis), indicates nanothread formation, with an estimated C…C distance of 2.5 Å estimated from refined lattice parameters (Fig. 1). This drop in the stacking cell length is accompanied by a simultaneous expansion of the *a*- axis, which is associated with H-bonding interactions. Interestingly, no corresponding change is

observed in the *b* axis which is also associated with the same H-bonding interactions. The lack of any notable change in the *b* axis suggests the preservation of carboxylate functionality, validating the H-bond stabilization hypothesis. Simultaneously, the sample transforms to an orange color, which has previously associated with the onset of nanothread polymerization.[18,22,23,32] Decreased compressibility observed at higher pressures is indicative of denser covalent materials, supporting nanothread formation. Single-crystal diffraction measurements of 2,5-FDCA are in good agreement with the powder data and show a clear splitting of Bragg peaks with the same symmetry indicating a polymerization-induced, single-crystal-to-single-crystal transformation (Fig. S2).

In situ FTIR measurements show the clear onset of chemical reaction near 13 GPa, confirming that the sharp decrease in volume observed by XRD is due to an irreversible chemical reaction. The FTIR spectrum of 2,5-FDCA collected at low pressure is in good agreement with previously studies, and no low-pressure, polymorphic phase transitions occur under compression.[43] Above ~14 GPa, several new peaks at *ca*. 1163, 1103, 899, and 717 cm^{-1} appear, followed by additional peaks at *ca*. 1510 and 1282 cm^{-1} above 17 GPa. Across the same pressure range, peaks corresponding to sp^2 C=C and C-H vibrations decrease dramatically in intensity, disappearing entirely above 19 GPa (Fig. S3). In situ Raman (Fig. S4) spectra also show a distinct loss of molecular vibrational modes above the reaction onset pressure, consistent with previously reported nanothread materials.[23,32]

PXRD of the recovered sample (Fig. 2A) shows the original lattice of molecular 2,5-FDCA, but with new structural packing indicative of nanothread formation. The preservation of crystalline long-range order to *d*-spacings below 2 Å upon decompression is in stark contrast to previously reported furan nanothreads, which exhibit significantly broadened diffraction upon recovery to ambient pressure.[20,21] We hypothesize that the enhanced stability provided by the hydrogen bonding network in 2,5-FDCA prevents structural rearrangement of the resulting nanothread polymer. The FTIR spectrum of the recovered material (Fig. 2B) also indicates a high degree of chemical homogeneity, exhibiting sharp, well-defined absorption features. Importantly, the presence of absorption bands at *ca.* 1742 and 1238 cm^{-1}, attributed to carboxylate C=O and C-O vibrations respectively, confirm retention of the carboxylic acid groups with minimal broadening. Notably, the shift in the C=O vibration to higher frequency indicates a change in the attached furan ring from an unsaturated to a saturated hydrocarbon, strongly supporting nanothread formation. For example, the C=O vibration in 2-furoic acid ($C_5H_4O_3$) occurs at *ca.* 1693 cm^{-1},[44] whereas the corresponding vibration in tetrahydro-2-furoic acid ($C_5H_8O_3$) appears at *ca.* 1748 cm^{-1}.[44] Ordered carboxylate O-H vibrations at *ca.* 3151 and 3125 cm^{-1} also shift to a broader singlet at *ca.* 3054 cm^{-1} indicating retention of the hydrogen bonding network in the resulting nanothread polymer. Due to the broad -OH vibrations above 3000 cm^{-1} we cannot directly monitor the formation of sp^3 C-H stretching vibrations which are usually used to indicate the onset of an intermolecular nanothread forming reaction. However, loss of the sp^2 C=C and C-H vibrations at *ca.* 1572 cm^{-1} and 962 cm^{-1} in the recovered material strongly support a change in hybridization of the furan backbone due to nanothread formation.

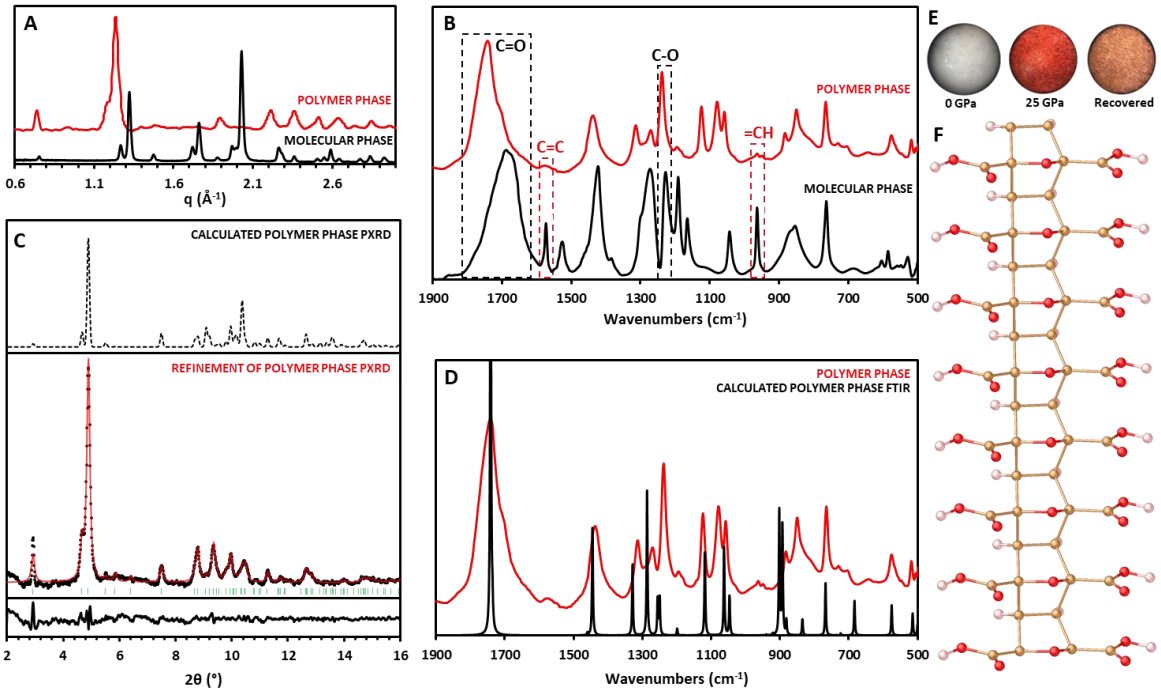

Figure 2. Structural and Spectroscopic Characterization of Nanothread Polymer Phase
A) Comparison of the integrated 1D XRD patterns for powder samples of 2,5-FDCA at 0 GPa (black), and after compression to 30 GPa (red); B) Comparison of the FTIR spectra for 2,5-FDCA at 0 GPa (black), and a sample recovered from compression to 24.5 GPa (red) between 700 – 2000 cm-1. Red boxes indicate peaks corresponding to sp2 C=C or C-H vibrations which are lost between samples. Black boxes indicate vibrations corresponding to carboxylate C=O and C-O vibrations which remain, indicating retention of carboxylate functionality; C) XRD pattern of syn-2,5-FDCA at 1 atm (black points) with Le Bail refinement (red) (λ = 0.4340 Å); D) Comparison of the experimental FTIR spectrum of syn-2,5-FDCA recovered after compression in a DAC (red), and the calculated (B3LYP) FTIR spectrum for the DFT-optimized structure of syn-2,5-FDCA. A scaling factor was applied to account for thermal expansion; E) Images of 2,5-FDCA collected during compression; F) Structure of the DFT-optimized nanothread polymer, syn-2,5-FDCA.

To confirm the structure of the recovered polymer, we optimized a packed 2,5-FDCA nanothread using DFT for direct comparison to experimental data (Fig 3A). While furan nanothreads have been found to form in the *anti* conformation[20,21] (i.e., oxygens alternate sides along the nanothread backbone) we optimized the 2,5-FDCA nanothread in the *syn* conformation (i.e., all oxygen atoms aligned along one side of the nanothread) due to the geometry of the starting material and the high energy penalty that would be incurred by the disruption of the hydrogen bonding network during the structural rearrangements required for other conformations. The calculated FTIR spectrum of the *syn* polymer (hereafter referred to as *syn*-2,5-FDCA) is an exceptional match with experimental data (Fig 3C). Notably, in this structure the peaks at *ca*. 1271 and 1238 cm^{-1} are assigned to sp^3 C-H wagging and sp^3 C-H bending vibrations respectively, further validating nanothread formation. Further assignment of the experimental IR spectrum can be found in Table S1. Similarly, Le Bail refinement of the lattice parameters for the DFT-optimized structure (Fig. 3B) indicates that this model is in good agreement with experimentally collected diffraction data at ambient conditions, accounting for thermal expansion of the calculated (0 K) cell. The structure indexes to a monoclinic lattice with cell parameters: a = 5.33 Å, b = 16.98 Å, c = 2.74 Å, and β = 87.92°. Furthermore, solid-state ^{13}C NMR of a sample synthesized in a Paris-Edinburgh (PE) press shows six well resolved peaks at 167, 165, 146, 124, 89 and 58 ppm. The sharp peaks at 165, 146 and 124 ppm are assigned to residual 2,5-FDCA, consistent with XRD and FTIR. The remaining, broader, peaks at 167, 89 and 58 ppm are assigned to sp^2 COOH, sp^3 O-C-COOH and sp^3 C-H respectively. The peaks assigned to sp^3 C are in reasonable agreement with "perfect" furan derived nanothreads which exhibits peaks at 77 (O-C-H) and 50 ppm (C-H), respectively.[20] Methanol washing was found to successfully remove any residual starting material, providing a simple route to the pure, chemically homogenous nanothread product.

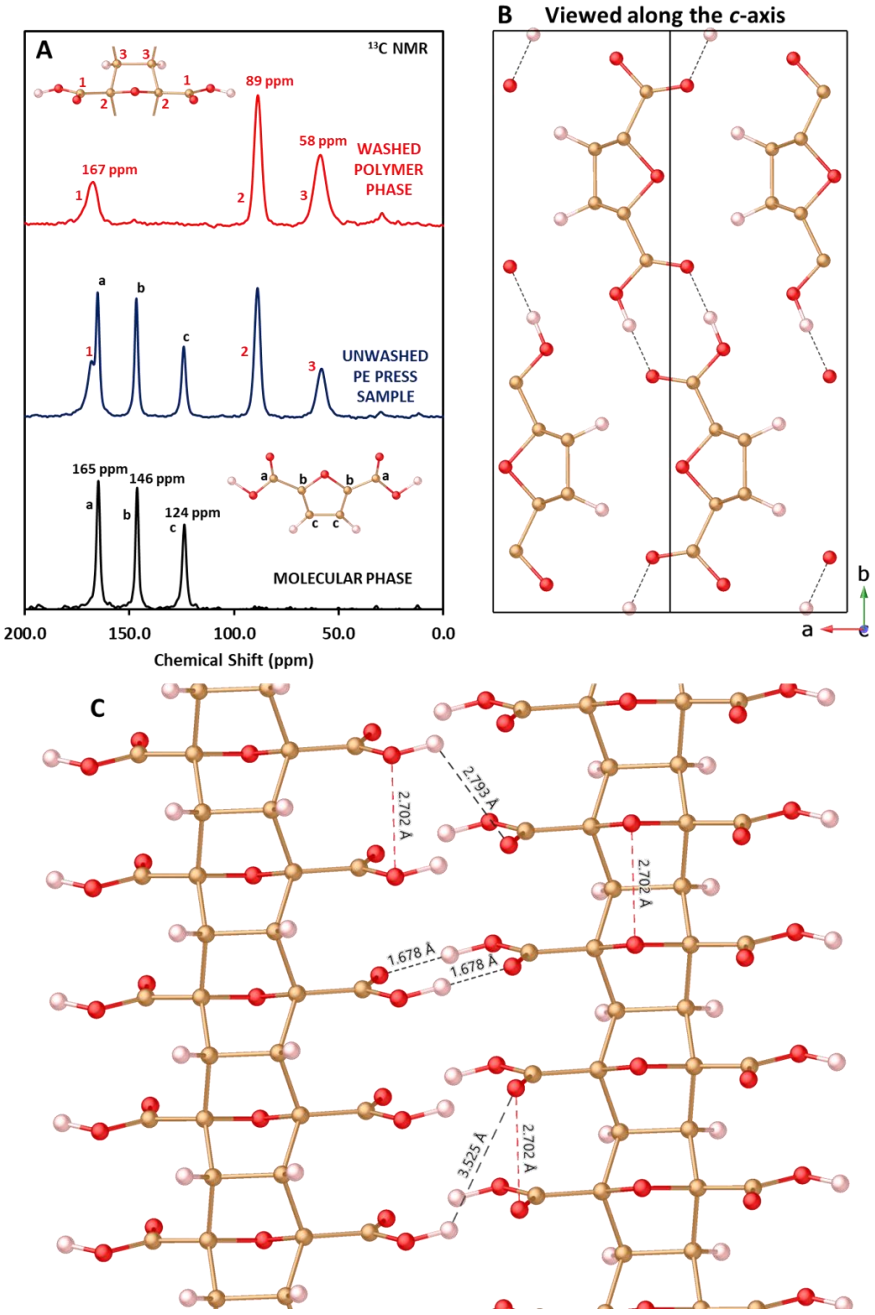

Figure 3. Analysis of C^{13}-NMR and Polymer Phase Structure
A) Comparison of the solid-state NMR spectra for 2,5-FDCA (black), a recovered, unwashed PE press sample (blue) which contains unreacted starting material (a, b ,c) along with polymer phase (1, 2, 3), and a washed PE press sample (red) which contains only polymer phase; B) View of the polymer phase of 2,5-FDCA along the molecular stacking c axis; C) Select intermolecular bond distances for two 2,5-FDCA nanothreads. Black dashed lines represent oxygen-hydrogen interactions, red dashed lines represent oxygen-oxygen interactions.

This chemically homogeneous, densely functionalized nanothread polymer represents a new kind of hydrogen-bonded organic framework (HOF) material,[45] currently of extreme interest due to their simple synthesis and unique gas uptake properties. As HOFs and other carboxylate-rich polymers such as poly(acrylic acid) are known to have unique sorption properties (e.g., superabsorbent water uptake), we

hypothesize that based on the structure of the nanothread polymer (Figure 3B/C), this material should also be extremely hydrophilic. Indeed, when the material is exposed to air it immediately begins to sorb ambient moisture. This sorption is accompanied by a color change from orange to white along with notable swelling of the material, consistent with the behavior of known superabsorbents (Fig. S5). Interestingly, when this sample is broken apart, the inner region of the sample which was not in direct contact with the atmosphere remains orange, indicating that water is slowly permeating the sample without the need for external stimulus. Time resolved XRD of *syn*-2,5-FDCA in the presence of ambient moisture shows that water sorption induces amorphization of the polymer (Fig. S6). Conversely, a sample stored under an inert argon atmosphere remains crystalline over the same time period. Water-sorption-induced amorphization of the polymer is not entirely unexpected, as it is highly unlikely that ambient water will incorporate into the polymer network in an ordered fashion. Time-resolved FT-IR studies of *syn*-2,5-FDCA also show an immediate change in the absorption spectra upon exposure to air, with the emergence of new vibrational modes (Fig. S7). At the same time several nanothread peaks decrease in intensity, most notably the peaks at 1440 and 1314 cm^{-1}, which correspond to C-O stretching and O-H wagging vibrations respectively. These spectral changes are coincident with the growth of a new, broad band at *ca*. 3434 cm^{-1}, clear evidence of water sorption by the polymer. Comparison of the FT-IR spectra of the samples used in time-resolved measurements and the sample used for solid-state NMR measurements are in excellent agreement (Fig. S8), demonstrating that there are no chemical changes to the nanothread backbone. The hydroscopic nature of the sample was confirmed by thermogravimetric analysis (TGA) which shows a 12.6 % mass loss below 100 °C characteristic of the loss of absorbed water. TGA analysis also shows a sharp 74.6 % mass loss starting at 282 °C, consistent with loss of carboxylates in 2,5-FDCA (Fig. 4C). The hydrophilic nature of this material warrants additional investigation for sorption of other gases and opens the possibility for novel separation and storage applications.

As the carboxylate groups in *syn*-2,5-FDCA are chemically accessible, we began to explore more complex bond forming transformations, thinking of the functionalized threads as unique synthons for additional post-processing. The ability to carry out chemical reactions on the surface of a nanothread, and therefore precisely tune their chemical and physical properties would mark a significant advancement in the ability to tailor these materials for use in advanced applications. Carboxylates are commonly used in a variety of organic (e.g., amide, ester formation) and inorganic (e.g., metal binding) reactions, and are integral to the formation and post-synthetic modification of advanced materials such as metal- and covalent-organic frameworks (MOFs/COFs).[46,47] The ability to bind metals to the surface of nanothread materials has been the focus of theoretical studies,[48] but has yet to be realized experimentally. Evidence of successful metal coordination would mark a significant advancement in the use of these materials as independent synthons, with the possibility to access unique materials properties[48] and potential to produce unique multidimensional frameworks using similar linker concepts used in MOFs.

To test the feasibility of producing metal-bound structures, samples of *syn*-2,5-FDCA were deprotonated and exposed to a variety of 3*d* transition metals commonly used in MOF formation (Fe^{3+}, Co^{2+}, Cu^{2+}, Zn^{2+}). Samples exposed to Fe, Co and Cu all show clear color changes that persist after multiple washes, suggesting permanent metal coordination (Fig. 4A). Solid-state ^{13}C-NMR collected on the sample exposed to Zn shows a shift in the carboxylate peak from 167 to 170 ppm (Fig. 4B), consistent with a carboxylate bound to a d^{10} metal (*cf*. 172 ppm in MOF-5 (Zn)[49], 171 ppm in UiO-66 (Zr)[50]). Such a change in the NMR spectra of *syn*-2,5-FDCA confirms successful metal binding to the nanothread backbone. Thermogravimetric analysis (TGA) of the same material exhibits two sharp decomposition features. The first, with onset of 280 °C, is consistent with thermally induced decarboxylation of free -COOH groups as discussed previously (Fig. 4C). This initial decomposition is then followed by a region of stability between 380 – 725 °C after which a second, decomposition event is observed. Similar TGA curves are commonly seen in multidimensional coordination polymers (e.g., MOFs).[51] Given the similarity to these materials, this result provides the first proof-of-concept to inspire research on the crosslinking of nanothreads to form multidimensional networks. TGA curves of the other metalated threads showed similar changes in the shape and onset temperature of thermal decomposition upon metal coordination (Fig. S9). Although the precise nature of metal binding is currently unknown, the case of *syn*-2,5-FDCA-Co clearly reveals the presence of open metal sites, which may be used for even further reaction and tailoring of chemical properties. Dry *syn*-2,5-FDCA-Co possesses a deep blue color, indicative of tetrahedral coordination geometry. When left in air it quickly changes to a pink color, indicative of an octahedral geometry caused by OH_2 coordination. This process can be reversed by simply heating the sample to drive off the water,

returning the material to its deep blue color. These materials are being investigated further for their use as a new class of sorbent polymers, given that systems with open metal sites have been shown to possess unique and unusual gas sorption and chemical sensing properties.[52-55]

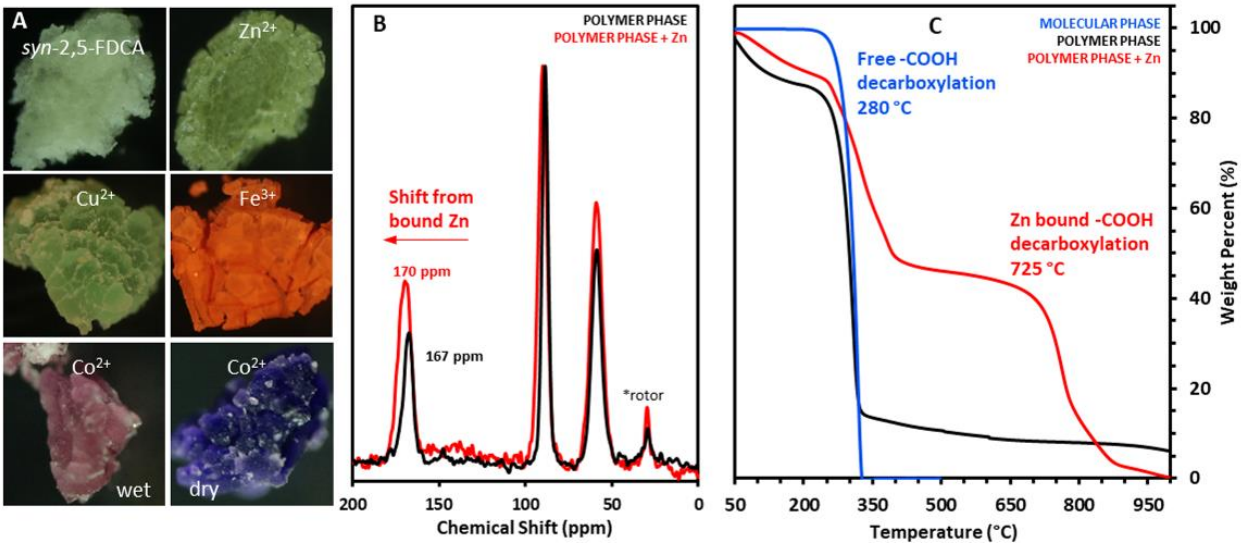

Figure 4. Post-synthetic metal coordination to *syn*-2,5-FDCA
A) Images showing samples of *syn*-2,5-FDCA before and after exposure to a variety of metal cations; B) Comparison of the solid-state ^{13}C NMR spectra for *syn*-2,5-FDCA before (black) and after exposure to Zn^{2+} cations (red). Note the shift in the COOH peak from 167-170 ppm indicating Zn binding; C) Comparison of the thermogravimetric analysis (TGA) curves for 2,5-FDCA (blue), *syn*-2,5-FDCA (black), and *syn*-2,5-FDCA-Zn (red).

In conclusion, we have shown how careful consideration of molecular stacking and intermolecular forces can be used to produce chemically homogeneous nanothread polymers via pressure-induced polymerization. Compression of 2,5-furanidcarboxylic acid to approximately 13 GPa induces a series of constrained [4 + 2] Diels Alder cycloaddition reactions, producing a chemically homogenous sp^3 furan backbone polymer that is functionalized with a high density of carboxylate groups. This polymer exhibits potential superabsorbent properties, readily absorbing ambient moisture without external stimulus. In addition, this material readily coordinates various 3*d* metal ions indicating the suitability of functionalized nanothreads to act as independent synthons for post-processing with the potential to produce novel multidimensional networks. These results signify the first example of deliberate, controlled *post*-synthetic modification of a nanothread, which may ultimately lead to the development of extended nanothread networks with a wide range of novel physical properties.

EXPERIMENTAL PROCEDURES

Resource availability

Further information and requests for resources should be directed to Samuel Dunning (sdunning@carnegiescience.edu) and/or Timothy Strobel (tstrobel@carnegiescience.edu).

Materials availability
All materials generated in this study are available from the lead contacts without restriction

Data and code availability
This study did not generate any datasets.

Chemicals

Commercially available 2,5-furandicarboxylic acid (2,5-FDCA, 98%; TCI), $ZnCl_2 \cdot xH_2O$ (99.99%, Alfa Aesar), $CoCl_2$ (99.7%, Alfa Aesar), $CuCl_2 \cdot 2H_2O$ (99+%, Alfa Aesar), $Fe(NO_3)_3 \cdot 9H_2O$ (98+%, Alfa Aesar),

NaOH (98%, Thermo Scientific), and methanol (99.8+%, Alfa Aesar) were used as received. For single-crystal studies, 2,5-FDCA was recrystallized from methanol by slow evaporation.

High Pressure Synthesis

Diamond anvil cells (DACs). For initial proof-of-concept work, DACs with 400 μm culets and rhenium gaskets were used. Re was pre-indented to ca. 40 μm before a ca. 180 μm hole was drilled through the center of the indentation. The hole in the Re gasket was used as the sample chamber. For in-situ FTIR/Raman measurements a ruby chip was added with the sample for in situ measurement of pressure within the DAC, estimated through ruby fluorescence. For in situ XRD measurements gold (Au) was added to the sample as a pressure calibrant. Powder samples of 2,5-FDCA were loaded directly into the sample chamber without any additional pressure transmitting medium. For single crystal measurements, neon was used as the pressure transmitting medium.

Paris-Edinburgh (PE) Press. Paris-Edinburgh (PE) press experiments were carried out using a VX3 Paris-Edinburgh press equipped with double-toroidal sintered diamond anvils. A Teledyne ISCO 30D Syringe Pump with a maximum pressure of 30,000 psi was used to drive the system. Samples were synthesized by packing 2,5-FDCA powder into a Ti (ELI grade) sample chamber and were pressurized to 24,000 psi in constant pressure mode. Samples were held at the desired pressure for 24 hours before decompression. The rate of compression and decompression are as follows: 1 mL/min below 1000 psi, 0.3 mL/min from 1000 to 5000 psi, 0.02 mL/min from 5000 to 20,000 psi, 0.01 mL/min from 20,000 psi to 24,000 psi.

Nanothread Purification and Post-Processing

Purification. PE Press samples were recovered from their Ti gaskets and suspended in an excess of methanol (2 mL). The samples were thoroughly sonicated using a Branson 200 Ultrasonic Cleaner. The samples were recovered by centrifugation using an IEC Centra CL2 and the supernatant was removed. This process was carried out in triplicate, and samples were placed in a Fisher Scientific Isotemp 282A oven set to 120 °C to dry.

Post-processing. All metal coordination studies were carried out using the same method. Washed samples of *syn*-2,5-FDCA were first deprotonated by exposure to a slight excess of 0.1 M $NaOH_{(aq)}$. The samples were recovered by centrifugation, and the supernatant was removed. The samples were then exposed to an excess of a 0.25 M methanolic solution of the respective metal salt. These samples were recovered, washed, and dried using the same process described in the previous section.

SUPPLEMENTAL INFORMATION

Supplemental information contains additional experimental procedures, Figures S1–S9, and Table S1

ACKNOWLEDGMENTS

Portions of this work were performed at GeoSoilEnviroCARS (The University of Chicago, Sector 13) Advanced Photon Source (APS), Argonne National Laboratory. GeoSoilEnviroCARS is supported by the National Science Foundation - Earth Sciences (EAR-1634415) and Department of Energy – GeoSciences (DE-FG02-94ER14466). This research used resources of the Advanced Photon Source; a U.S. Department of Energy (DOE) Office of Science User Facility operated for the DOE Office of Science by Argonne National Laboratory under Contract DE-AC02- 06CH11357.

The authors acknowledge funding support from The Arnold and Mabel Beckman Foundation (Arnold O. Beckman Postdoctoral Fellowship in Chemical Sciences Program) and the U.S. Army Research Office (Grant W911NF-17-1-0604).

AUTHOR CONTRIBUTIONS

SGD and TAS: Project conceptualization, sample synthesis, purification, characterization. High pressure FTIR, Raman and XRD data collection.
LZ and BC: Theoretical calculations. GDC: Solid-state 13C NMR studies.
GDC: Solid-state NMR studies
DZ, SC, VBP: Assistance in high pressure XRD data collection.

DECLARATION OF INTERESTS

The authors declare no competing interests.

REFRENCES

1 Rodil, S. E., Ferrari, A. C., Robertson, J. & Milne, W. I. Raman and infrared modes of hydrogenated amorphous carbon nitride. *Journal of Applied Physics* **89**, 5425-5430, doi:10.1063/1.1365076 (2001).

2 Citroni, M. *et al.* Structural and Electronic Competing Mechanisms in the Formation of Amorphous Carbon Nitride by Compressing s-Triazine. *Journal of Physical Chemistry C* **119**, 28560-28569, doi:10.1021/acs.jpcc.5b09538 (2015).

3 Zhu, T. S. & Ertekin, E. Phonons, Localization, and Thermal Conductivity of Diamond Nanothreads and Amorphous Graphene. *Nano Letters* **16**, 4763-4772, doi:10.1021/acs.nanolett.6b00557 (2016).

4 Gou, H. Y. *et al.* Pressure-induced polymerization of P(CN)(3). *Journal of Chemical Physics* **142**, 194503, doi:10.1063/1.4919640 (2015).

5 Keefer, D. W. *et al.* Pressure-Induced Polymerization of LiN(CN)(2). *Journal of Physical Chemistry A* **120**, 9370-9377, doi:10.1021/acs.jpca.6b06780 (2016).

6 Keefer, D. W. *et al.* Tetracyanomethane under Pressure: Extended CN Polymers from Precursors with Built-in sp(3) Centers. *Journal of Physical Chemistry A* **122**, 2858-2863, doi:10.1021/acs.jpca.7b10729 (2018).

7 Li, F., Xu, J., Wang, Y., Zheng, H. & Li, K. Pressure-Induced Polymerization: Addition and Condensation Reactions. *Molecules* **26**, 7581 (2021).

8 Yang, X., Wang, X., Wang, Y., Li, K. & Zheng, H. From Molecules to Carbon Materials—High Pressure Induced Polymerization and Bonding Mechanisms of Unsaturated Compounds. *Crystals* **9**, 490 (2019).

9 Biradha, K. & Santra, R. Crystal engineering of topochemical solid state reactions. *Chemical Society Reviews* **42**, 950-967, doi:10.1039/C2CS35343A (2013).

10 Wang, G.-W. Mechanochemical organic synthesis. *Chemical Society Reviews* **42**, 7668-7700, doi:10.1039/C3CS35526H (2013).

11 Ward, M. D., Huang, H. T., Zhu, L., Popov, D. & Strobel, T. A. High-Pressure Behavior of C2I2 and Polymerization to a Conductive Polymer. *Journal of Physical Chemistry C* **123**, 11369-11377, doi:10.1021/acs.jpcc.8b12161 (2019).

12 Huang, H. T. *et al.* Nanoarchitecture through Strained Molecules: Cubane-Derived Scaffolds and the Smallest Carbon Nanothreads. *Journal of the American Chemical Society* **142**, 17944-17955, doi:10.1021/jacs.9b12352 (2020).

13 Romi, S., Fanetti, S., Alabarse, F. & Bini, R. Structure–Reactivity Relationship in the High-Pressure Formation of Double-Core Carbon Nanothreads from Azobenzene Crystal. *J. Phys. Chem. C* **125**, 17174-17182, doi:10.1021/acs.jpcc.1c04003 (2021).

14 Romi, S., Fanetti, S., Alabarse, F. G., Bini, R. & Santoro, M. High-Pressure Synthesis of 1D Low-Bandgap Polymers Embedded in Diamond-like Carbon Nanothreads. *Chemistry of Materials* **34**, 2422-2428, doi:10.1021/acs.chemmater.1c04453 (2022).

15 Romi, S. *et al.* Towards custom built double core carbon nanothreads using stilbene and pseudo-stilbene type systems. *Nanoscale* **14**, 4614-4625, doi:10.1039/D1NR08188H (2022).

16 Zhu, L. *et al.* Carbon-boron clathrates as a new class of sp³-bonded framework materials. *Science Advances* **6**, eaay8361, doi:doi:10.1126/sciadv.aay8361 (2020).

17 Fitzgibbons, T. C. *et al.* Benzene-derived carbon nanothreads. *Nature Materials* **14**, 43-47, doi:10.1038/nmat4088 (2015).

18 Ward, M. D. *et al.* Controlled Single-Crystalline Polymerization of $C_{10}H_8 \cdot C_{10}F_8$ under Pressure. *Macromolecules* **52**, 7557-7563, doi:10.1021/acs.macromol.9b01416 (2019).

19 Gerthoffer, M. C. *et al.* 'Sacrificial' supramolecular assembly and pressure-induced polymerization: toward sequence-defined functionalized nanothreads. *Chemical Science* **11**, 11419-11424, doi:10.1039/d0sc03904g (2020).

20 Matsuura, B. S. *et al.* Perfect and Defective C-13-Furan-Derived Nanothreads from ModestPressure Synthesis Analyzed by C-13 NMR. *Journal of the American Chemical Society* **143**, 9529-9542, doi:10.1021/jacs.1c03671 (2021).

21 Huss, S. *et al.* Scalable Synthesis of Crystalline One-Dimensional Carbon Nanothreads through Modest-Pressure Polymerization of Furan. *Acs Nano* **15**, 4134-4143, doi:10.1021/acsnano.0c10400 (2021).

22 Biswas, A. *et al.* Evidence for Orientational Order in Nanothreads Derived from Thiophene. *Journal of Physical Chemistry Letters* **10**, 7164-7171, doi:10.1021/acs.jpclett.9b02546 (2019).

23 Dunning, S. G. *et al.* Solid-State Pathway Control via Reaction-Directing Heteroatoms: Ordered Pyridazine Nanothreads through Selective Cycloaddition. *Journal of the American Chemical Society* **144**, 2073-2078, doi:10.1021/jacs.1c12143 (2022).

24 Gao, D. *et al.* Crystalline $C_3N_3H_3$ tube (3,0) nanothreads. *Proceedings of the National Academy of Sciences* **119**, e2201165119, doi:doi:10.1073/pnas.2201165119 (2022).

25 Zhan, H. F. & Gu, Y. T. *Thermal Conductivity of Diamond Nanothread*. (2017).

26 Silveira, J. & Muniz, A. R. First-principles calculation of the mechanical properties of diamond nanothreads. *Carbon* **113**, 260-265, doi:10.1016/j.carbon.2016.11.060 (2017).

27 Zhang, L. W., Ji, W. M. & Liew, K. M. Mechanical properties of diamond nanothread reinforced polymer composites. *Carbon* **132**, 232-240, doi:10.1016/j.carbon.2018.02.053 (2018).

28 Zhan, H. F. & Gu, Y. T. Thermal conduction of one-dimensional carbon nanomaterials and nanoarchitectures. *Chinese Physics B* **27**, doi:10.1088/1674-1056/27/3/038103 (2018).

29 Xue, Y. X. *et al.* Strain engineering for thermal conductivity of diamond nanothread forests. *Journal of Physics D-Applied Physics* **52**, doi:10.1088/1361-6463/aaf559 (2019).

30 Wang, P., Zhan, H. F. & Gu, Y. T. Molecular Dynamics Simulation of Chiral Carbon Nanothread Bundles for Nanofiber Applications. *Acs Applied Nano Materials* **3**, 10218-10225, doi:10.1021/acsanm.0c02183 (2020).

31 Li, X. *et al.* Mechanochemical Synthesis of Carbon Nanothread Single Crystals. *Journal of the American Chemical Society* **139**, 16343-16349, doi:10.1021/jacs.7b09311 (2017).

32 Li, X. *et al.* Carbon Nitride Nanothread Crystals Derived from Pyridine. *Journal of the American Chemical Society* **140**, 4969-4972, doi:10.1021/jacs.7b13247 (2018).

33 Roman, R. E., Kwan, K. & Cranford, S. W. Mechanical Properties and Defect Sensitivity of Diamond Nanothreads. *Nano Letters* **15**, 1585-1590, doi:10.1021/nl5041012 (2015).

34 Zhan, H. F. *et al.* From brittle to ductile: a structure dependent ductility of diamond nanothread. *Nanoscale* **8**, 11177-11184, doi:10.1039/c6nr02414a (2016).

35 Tang, W. S. & Strobel, T. A. Evidence for Functionalized Carbon Nanothreads from pi-Stacked, para-Disubstituted Benzenes. *Journal of Physical Chemistry C* **124**, 25062-25070, doi:10.1021/acs.jpcc.0c06715 (2020).

36 van der Lubbe, S. C. C. & Guerra, C. F. The Nature of Hydrogen Bonds: A Delineation of the Role of Different Energy Components on Hydrogen Bond Strengths and Lengths. *Chemistry-an Asian Journal* **14**, 2760-2769, doi:10.1002/asia.201900717 (2019).

37 Ballatore, C., Huryn, D. M. & Smith III, A. B. Carboxylic Acid (Bio)Isosteres in Drug Design. *ChemMedChem* **8**, 385-395, doi:https://doi.org/10.1002/cmdc.201200585 (2013).

38 Zohuriaan, J. & Kabiri, K. Superabsorbent Polymer Materials: A Review. *Iranian Polymer Journal (English Edition)* **17** (2008).

39 Zhou, H.-C., Long, J. R. & Yaghi, O. M. Introduction to Metal–Organic Frameworks. *Chem. Rev.* **112**, 673-674, doi:10.1021/cr300014x (2012).

40 del Olmo, A., Calzada, J. & Nunez, M. Benzoic acid and its derivatives as naturally occurring compounds in foods and as additives: Uses, exposure, and controversy. *Critical Reviews in Food Science and Nutrition* **57**, 3084-3103, doi:10.1080/10408398.2015.1087964 (2017).

41 Zhu, Z. *et al.* Modular Design of Chiral Conjugate-Base-Stabilized Carboxylic Acids: Catalytic Enantioselective [4 + 2] Cycloadditions of Acetals. *Journal of the American Chemical Society* **142**, 15252-15258, doi:10.1021/jacs.0c07212 (2020).

42 Martuscelli, E. & Pedone, C. Crystal and molecular structure of furane-alpha,alpha'-dicarboxylic acid. *Acta Crystallographica Section B-Structural Crystallography and Crystal Chemistry* **B 24**, 175-179, doi:10.1107/s0567740868001901 (1968).

43 Zhang, S. & Zhang, L. A facile and effective method for preparation of 2.5-furandicarboxylic acid via hydrogen peroxide direct oxidation of 5-hydroxymethylfurfural. *Polish Journal of Chemical Technology* **19**, 11-16, doi:10.1515/pjct-2017-0002 (2017).

44 NIST Mass Spectrometry Data Center, W. E. W., director. in *NIST Chemistry WebBook, NIST Standard Reference Database Number 69* (ed P.J. Linstrom and W.G. Mallard) Ch. Infrared Spectra, (National Institute of Standards and Technology).
45 Li, P., Ryder, M. R. & Stoddart, J. F. Hydrogen-Bonded Organic Frameworks: A Rising Class of Porous Molecular Materials. *Accounts of Materials Research* **1**, 77-87, doi:10.1021/accountsmr.0c00019 (2020).
46 Furukawa, H., Cordova, K. E., O'Keeffe, M. & Yaghi, O. M. The Chemistry and Applications of Metal-Organic Frameworks. *Science* **341**, 1230444, doi:10.1126/science.1230444 (2013).
47 Mandal, S., Natarajan, S., Mani, P. & Pankajakshan, A. Post-Synthetic Modification of Metal-Organic Frameworks Toward Applications. *Advanced Functional Materials* **31**, doi:10.1002/adfm.202006291 (2021).
48 Miao, Z. Z., Cao, C., Zhang, B., Duan, H. M. & Long, M. Q. Effects of 3d-transition metal doping on the electronic and magnetic properties of one-dimensional diamond nanothread. *Chinese Physics B* **29**, doi:10.1088/1674-1056/ab84dd (2020).
49 Bennabi, S. B., M. Synthesis and Characterization of a new hybrid material (MOF-5/Mag-H+) based on a Metal-Organic Framework and a Proton Exchanged Montmorillonite Clay (Maghnite-H+) as catalytic support. *Journal of Materials and Environmental Sciences* **8**, 4391-4398, doi:10.26872/jmes.2017.8.12.463 (2017).
50 Devautour-Vinot, S. *et al.* Structure and Dynamics of the Functionalized MOF Type UiO-66(Zr): NMR and Dielectric Relaxation Spectroscopies Coupled with DFT Calculations. *Chemistry of Materials* **24**, 2168-2177, doi:10.1021/cm300863c (2012).
51 Cavka, J. H. *et al.* A New Zirconium Inorganic Building Brick Forming Metal Organic Frameworks with Exceptional Stability. *Journal of the American Chemical Society* **130**, 13850-13851, doi:10.1021/ja8057953 (2008).
52 Li, Y.-W. *et al.* Microporous metal–organic frameworks with open metal sites as sorbents for selective gas adsorption and fluorescence sensors for metal ions. *Journal of Materials Chemistry A* **1**, 495-499, doi:10.1039/C2TA00635A (2013).
53 Perry, J. J. *et al.* Noble Gas Adsorption in Metal–Organic Frameworks Containing Open Metal Sites. *J. Phys. Chem. C* **118**, 11685-11698, doi:10.1021/jp501495f (2014).
54 Dunning, S. G. *et al.* A Sensor for Trace H2O Detection in D2O. *Chem* **2**, 579-589, doi:10.1016/j.chempr.2017.02.010 (2017).
55 Kökçam-Demir, Ü. *et al.* Coordinatively unsaturated metal sites (open metal sites) in metal–organic frameworks: design and applications. *Chemical Society Reviews* **49**, 2751-2798, doi:10.1039/C9CS00609E (2020).